

# Customized eye models for determining optimized intraocular lenses power

Carmen Canovas<sup>1,2,\*</sup> and Pablo Artal<sup>1</sup>

<sup>1</sup>Laboratorio de Óptica, Instituto Universitario de Investigación en Óptica y Nanofísica, Universidad de Murcia, Campus de Espinardo (Edificio 34), 30100 Murcia, Spain

<sup>2</sup>AMO Groningen B.V., Van Swietenlaan 5, 9728NX, Groningen, The Netherlands

\*Carmen.Canovas@amo.abbott.com

**Abstract:** We have developed a new optical procedure to determine the optimum power of intraocular lenses (IOLs) for cataract surgery. The procedure is based on personalized eye models, where biometric data of anterior corneal shape and eye axial length are used. A polychromatic exact ray-tracing through the surfaces defining the eye model is performed for each possible IOL power and the area under the radial MTF is used as a metric. The IOL power chosen by the procedure maximizes this parameter. The IOL power for 19 normal eyes has been determined and compared with standard regression-based predictions. The impact of the anterior corneal monochromatic aberrations and the eye's chromatic aberration on the power predictions has been studied, being significant for those eyes with severe monochromatic aberrations, such as post-LASIK cataract patients, and for specific IOLs with low Abbe numbers.

©2011 Optical Society of America

**OCIS codes:** (170.4460) Ophthalmic optics and devices; (330.5370) Physiological optics.

---

## References and links

1. W. J. Dupps, Jr., "Intraocular lens calculations: call for more deterministic models," *J. Cataract Refract. Surg.* **36**(9), 1447–1448 (2010).
2. W. Haigis, "Intraocular lens calculation in extreme myopia," *J. Cataract Refract. Surg.* **35**(5), 906–911 (2009).
3. K. J. Hoffer, "Intraocular lens power calculation for eyes after refractive keratotomy," *J. Refract. Surg.* **11**(6), 490–493 (1995).
4. A. Guirao, M. Redondo, E. Geraghty, P. Piers, S. Norrby, and P. Artal, "Corneal optical aberrations and retinal image quality in patients in whom monofocal intraocular lenses were implanted," *Arch. Ophthalmol.* **120**(9), 1143–1151 (2002).
5. J. T. Holladay, P. A. Piers, G. Koranyi, M. van der Mooren, and N. E. Norrby, "A new intraocular lens design to reduce spherical aberration of pseudophakic eyes," *J. Refract. Surg.* **18**(6), 683–691 (2002).
6. J. Tabernero, P. Piers, and P. Artal, "Intraocular lens to correct corneal coma," *Opt. Lett.* **32**(4), 406–408 (2007).
7. J. Tabernero, P. Piers, A. Benito, M. Redondo, and P. Artal, "Predicting the optical performance of eyes implanted with IOLs to correct spherical aberration," *Invest. Ophthalmol. Vis. Sci.* **47**(10), 4651–4658 (2006).
8. W. Haigis, "The Haigis formula," in *Intraocular Lens power calculations*, J. Shammas, ed. (Slack Incorporated, 2004).
9. K. J. Hoffer, "The Hoffer Q formula: a comparison of theoretic and regression formulas," *J. Cataract Refract. Surg.* **19**(6), 700–712 (1993).
10. J. T. Holladay, T. C. Prager, T. Y. Chandler, K. H. Musgrove, J. W. Lewis, and R. S. Ruiz, "A three-part system for refining intraocular lens power calculations," *J. Cataract Refract. Surg.* **14**(1), 17–24 (1988).
11. J. A. Retzlaff, D. R. Sanders, and M. C. Kraff, "Development of the SRK/T intraocular lens implant power calculation formula," *J. Cataract Refract. Surg.* **16**(3), 333–340 (1990).
12. J. Shammas, "Basic optics for intraocular lens power calculations," in *Intraocular Lens Power Calculations*, J. Shammas, ed. (Slack Incorporated, 2004).
13. P. C. Hoffmann and W. W. Hütz, "Analysis of biometry and prevalence data for corneal astigmatism in 23,239 eyes," *J. Cataract Refract. Surg.* **36**(9), 1479–1485 (2010).
14. S. Norrby, "Using the lens haptic plane concept and thick-lens ray tracing to calculate intraocular lens power," *J. Cataract Refract. Surg.* **30**(5), 1000–1005 (2004).
15. T. Olsen, "The Olsen formula," in *Intraocular Lens Power Calculations*, Shammas J, ed. (Slack Incorporated, 2004).

16. P. R. Preussner, J. Wahl, H. Lahdo, B. Dick, and O. Findl, "Ray tracing for intraocular lens calculation," *J. Cataract Refract. Surg.* **28**(8), 1412–1419 (2002).
17. P. R. Preussner, T. Olsen, P. Hoffmann, and O. Findl, "Intraocular lens calculation accuracy limits in normal eyes," *J. Cataract Refract. Surg.* **34**(5), 802–808 (2008).
18. S. Norrby, "The Dubbelman eye model analysed by ray tracing through aspheric surfaces," *Ophthalmic Physiol. Opt.* **25**(2), 153–161 (2005).
19. S. Norrby, "Sources of error in intraocular lens power calculation," *J. Cataract Refract. Surg.* **34**(3), 368–376 (2008).
20. E. Moreno-Barriuso, J. M. Lloves, S. Marcos, R. Navarro, L. Llorente, and S. Barbero, "Ocular aberrations before and after myopic corneal refractive surgery: LASIK-induced changes measured with laser ray tracing," *Invest. Ophthalmol. Vis. Sci.* **42**(6), 1396–1403 (2001).
21. A. Benito, M. Redondo, and P. Artal, "Laser in situ keratomileusis disrupts the aberration compensation mechanism of the human eye," *Am. J. Ophthalmol.* **147**(3), 424–431e1 (2009).
22. H. J. Shamma, M. C. Shamma, A. Garabet, J. H. Kim, A. Shamma, and L. LaBree, "Correcting the corneal power measurements for intraocular lens power calculations after myopic laser in situ keratomileusis," *Am. J. Ophthalmol.* **136**(3), 426–432 (2003).
23. J. Aramberri, "Intraocular lens power calculation after corneal refractive surgery: double-K method," *J. Cataract Refract. Surg.* **29**(11), 2063–2068 (2003).
24. P. R. Preussner, J. Wahl, and D. Weitzel, "Topography-based intraocular lens power selection," *J. Cataract Refract. Surg.* **31**(3), 525–533 (2005).
25. A. Guirao and P. Artal, "Corneal wave aberration from videokeratography: accuracy and limitations of the procedure," *J. Opt. Soc. Am. A* **17**(6), 955–965 (2000).
26. P. Rosales and S. Marcos, "Customized computer models of eyes with intraocular lenses," *Opt. Express* **15**(5), 2204–2218 (2007).
27. S. Barbero, S. Marcos, J. Merayo-Lloves, and E. Moreno-Barriuso, "A validation of the estimation of corneal aberrations from videokeratography: test on keratoconus eyes," *J. Refract. Surg.* **18**, 267–270 (2002).
28. Y. Le Grand and S. G. El Hage, *Physiological Optics* (Springer-Verlag, 1980).
29. T. Olsen, "On the calculation of power from curvature of the cornea," *Br. J. Ophthalmol.* **70**(2), 152–154 (1986).
30. M. Dubbelman, V. A. Sicam, and G. L. Van der Heijde, "The shape of the anterior and posterior surface of the aging human cornea," *Vision Res.* **46**(6-7), 993–1001 (2006).
31. T. Olsen, "Calculation of intraocular lens power: a review," *Acta Ophthalmol. Scand.* **85**(5), 472–485 (2007).
32. A. van Meeteren, "Calculations of the optical modulation transfer function of the human eye for white light," *Opt. Acta (Lond.)* **21**, 395–412 (1974).
33. P. Artal, A. Benito, and J. Tabernero, "The human eye is an example of robust optical design," *J. Vis.* **6**(1), 1–7 (2006).
34. P. Artal and J. Tabernero, "The eye's aplanatic answer," *Nat. Photonics* **2**(10), 586–589 (2008).
35. P. Artal, S. Manzanera, P. Piers, and H. Weeber, "Visual effect of the combined correction of spherical and longitudinal chromatic aberrations," *Opt. Express* **18**(2), 1637–1648 (2010).
36. H. Zhao and M. A. Mainster, "The effect of chromatic dispersion on pseudophakic optical performance," *Br. J. Ophthalmol.* **91**(9), 1225–1229 (2007).
37. I. De Loewenfeld, "Pupillary changes related to age," in *Topics in Neuro-ophthalmology*, H. S. Thompson, ed. (Williams & Wilkins, Baltimore, 1979), pp. 124–150.
38. S. Norrby, E. Lydahl, G. Koranyi, and M. Taube, "Clinical application of the lens haptic plane concept with transformed axial lengths," *J. Cataract Refract. Surg.* **31**(7), 1338–1344 (2005).
39. S. Norrby, O. Findl, N. Hirschschall, Y. Nishi, and R. Bergman, "Modeling the pseudo-phakic eye for the purpose of spherocylindrical IOL power calculation," presented at ARVO annual meeting, Fort Lauderdale, Fla., May 2–6, 2010.
40. S. Norrby, E. Lydahl, G. Koranyi, and M. Taube, "Reduction of trend errors in power calculation by linear transformation of measured axial lengths," *J. Cataract Refract. Surg.* **29**(1), 100–105 (2003).
41. A. Guirao, J. Tejedor, and P. Artal, "Corneal aberrations before and after small-incision cataract surgery," *Invest. Ophthalmol. Vis. Sci.* **45**(12), 4312–4319 (2004).

---

## 1. Introduction

The selection of the appropriate power of intraocular lenses (IOL) remains a challenge in cataract surgery [1]. This apparently simple problem from a theoretical optics point of view, becomes complicated when is applied in patients [2], especially in those that have undergone a previous refractive surgery [3]. The inaccuracy in the calculation affects the new types of IOLs with the potential of correcting different aberrations [4–6], due to the fact that errors in defocus larger than 0.5 D may reduce the potential visual benefit of correcting high order aberrations [7].

With respect to IOL power calculation, several approaches have been used. Currently, the most popular formulas [8–11] are those based on thin lens theory. In these formulas, the eye is

reduced to a two lens system, where the cornea is defined by a unique spherical surface and an equivalent refractive index, and the IOL is considered a thin lens [12]. The main differences between the common formulas arise from the calculation of the effective lens position. This was originally defined as the position of the principal plane of the thin IOL, which does not correspond with the real IOL position in the eye [10]. Hoffer [9], Holladay [10] and Retzlaff et al. [11] considered the axial length and corneal power as biometric inputs to predict this position. Haigis [8] also introduced the anterior chamber depth. In addition to these biometric terms, the most important parameter for the prediction methods is the IOL constant. This value, initially depending on the type of IOL and its characteristics, is now a fudged parameter used also to consider the biometric unit, lens placement and surgical technique [10]. These constants are globally optimized to improve results but an additional surgeon personalization is required in order to achieve the best performance of these formulas. Because of the regressive nature of this procedure and the variations in ocular configurations [13], these calculations cannot be considered accurate for all types of patients.

Other studies have presented IOL power calculation procedures based on thick lens theory [14,15]. Olsen [15] developed a formula based on paraxial thick lens ray tracing, where the position of the IOL was estimated by means of 5 biometric parameters. Still though, the paraxial nature of this formula did not consider corneal and IOL aberrations, limiting its accuracy. Preussner et al. [16] proposed the use of nonparaxial ray tracing procedures for IOL power calculations, showing specifically the importance of corneal asphericity, confirmed by a large population study [17] where average anterior corneal eccentricity values were used. Norrby [18] developed another thick-lens ray tracing procedure that considers spherical aberration. An analysis of all the errors affecting IOL power calculation was also performed considering the same tool [19], achieving a mean absolute error of 0.4D, equivalent to that associated to regular regression formulas in normal cases. As has been previously discussed, the average error is low for these formulas because the constants have been optimized for average effects, while considering thick lens theory or ray tracing, all considered distances are real, with no fudge parameters, being more evident the impact of measurement errors. However IOL power calculation should be improved to reduce not the average error but the error on an individual level. Therefore, the procedure should be further personalized for individual cases.

The inaccuracy of IOL power calculations in post-LASIK eyes is well established. It is important to note that considering corneal aberrations is particularly important for these patients, since it is well known that LASIK may alter and induce corneal aberrations [20,21]. There have been attempts to compensate for these inaccuracies with regressions based on other post-LASIK patients [22] or with the individual patient's preoperative data [23] which is not available in all the cases. However, these approaches are not yet fully accurate. In a step further in this direction, personalized corneal eccentricities, calculated from anterior corneal topography, were introduced in the nonparaxial ray tracing procedure [24], showing its influence in the calculation, especially for post-LASIK patients. The effect of the rest of anterior corneal aberrations was not considered in the calculation, although visual impression was generated to judge subjectively their impact.

Several tools are available for providing a better optical description of the eye. These tools should be used to improve and individualize IOL power calculations based in a complete description of corneal aberrations [25] and polychromatic estimations.

In this work, we present a fully customized procedure for IOL power calculations, based on a polychromatic exact ray-tracing performed for 4-mm pupil through an eye model built up from personalized optical and geometrical measurements. Because corneal topography is used to represent the anterior cornea, all aberrations present in subject's anterior cornea are considered in the prediction. The impact of anterior corneal aberrations and the differences between this procedure and some regression formulas are analyzed by means of the IOL power prediction performed for 19 normal healthy subjects.

## 2. Methods

### 2.1. IOL power calculation procedure

In order to generate a prediction of the eye's performance, different biometric data (anterior corneal topography, ocular axial length and anterior chamber depth) were measured prior to the surgery and introduced into the calculation procedure in order to allow for customization. Figure 1 shows a schematic view of the complete procedure. All the surfaces introduced in the model correspond to those in the real patient's eye. Here, we sequentially describe the surfaces considered in the customized eye model from the cornea to the retina.

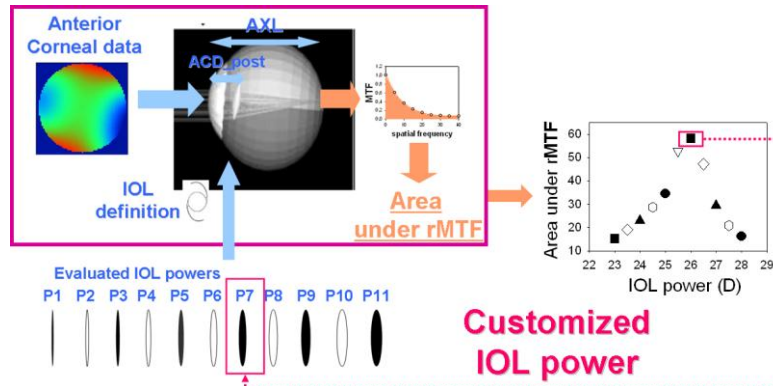


Fig. 1. Schematic diagram of the customized modeling for predicting IOL power. For every IOL power, an eye model is built from patient's biometric data from which the area under the radial MTF is retrieved, being chosen the IOL power that maximizes this metric.

The anterior corneal surface is introduced as a Zernike representation of the fitted elevation map obtained from the elevation data from a Placido based corneal topographer (Atlas; Carl Zeiss Meditec, Dublin CA, USA). Since the topographer provides corneal elevations in polar coordinates, in order to generate an adequate input for the used ray-tracing software (ZEMAX Development Corp, Bellevue, WA, USA) which requires data in rectangular coordinates, we pre-processed this raw data by using a least square fitting procedure to the eighth order Zernike expansion for an aperture diameter of 7-mm. This area was chosen as optimal because the fitted surface should be larger than the analyzed area in the eye model and should also avoid edge effects in the adjustment and throughout the ray tracing procedure. In addition, since we chose a 4-mm pupil size for the image quality calculations in the eye, we consider a 7-mm corneal aperture to be a suitable value. From this fitted surface, a regular grid of points in Cartesian coordinates is retrieved, as required for surface representation in the mentioned ray tracing software. This is a similar procedure to that described elsewhere [7,26] which retrieves similar results to some other procedures [25]. In addition, the reconstructed surface is re-centered with respect to the pupil by using decentration values between corneal apex and subject's pupil center.

The surfaces representing anterior corneas can also be used to calculate anterior corneal aberrations in a separate model through which ray tracing can be performed. In this case, the focal distance is set in order to minimize the root-mean-square spot size at the image plane since it has been shown as an accurate procedure [27]. The calculation of anterior corneal aberrations is an important preliminary step in the procedure because it is used to evaluate the anterior corneal topographies that are going to be used in the IOL power prediction. Aberration differences among various independent topographies help to understand possible changes in the final estimation of the IOL power.

We considered the contribution of the posterior cornea by using an equivalent refractive index for the anterior surface. This equivalent refractive index is determined to achieve the power of the complete cornea in the Legendre's eye model [28] while only considering the

anterior surface of the cornea by the use of a similar procedure to that described by Olsen et al. [29]. The resultant value 1.33 agrees well with the value previously calculated from anatomical data [30]. Because our procedure is performed in polychromatic light, we use the dispersion values of water for modeling the dispersion of that equivalent refractive index. The axial position of the pupil of the system was set in the same position as the anterior chamber depth prior to the surgery, considered as the distance between the anterior cornea and the anterior surface of the lens.

The prediction of the IOL position after the surgery is especially relevant for the calculations [19], especially relevant for short eyes [31]. Although whatever algorithm predicting actual lens position can be used in this customized procedure, we decided to use the relationship between the anterior chamber depth prior to the surgery ( $ACD_{pre}$ ), measured with anterior segment slit-lamp images (IOL Master; Carl Zeiss Meditec, Jena, Germany) and the actual IOL position measured from the anterior cornea (called anterior chamber depth after the surgery ( $ACD_{post}$ )) measured with an anterior chamber OCT instrument (Visante, Carl Zeiss Meditec, Dublin, CA) found in a previous study (Fig. 2). The relationship between these two parameters was linear (Eq. (1)) with a high degree of correlation ( $r^2 = 0.8$ ).

$$ACD_{post} = 0.88 \times ACD_{pre} + 1.63 \quad (1)$$

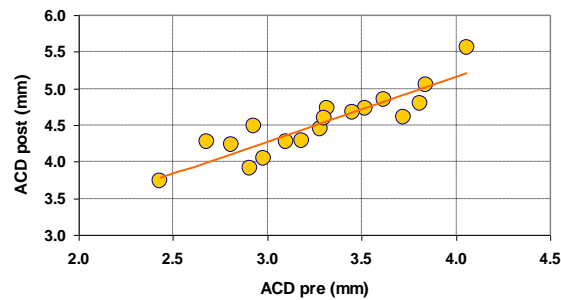


Fig. 2. Anterior chamber depth prior to the surgery as function of the anterior chamber depth after the surgery. From this result, we extracted the predictive model described by Eq. (1).

The particular geometry of the IOL (surfaces radius and asphericity terms, thickness) and its optical properties (refractive index and dispersion) should be introduced into the model. All IOL types and designs can be considered if these design parameters are known.

If a spherical lens is used, the calculation is performed at the circle of least confusion by correcting corneal astigmatism in the eye model. To perform this correction, we introduce a surface containing the opposite amount of both components of corneal astigmatism (we call this  $-A$  in diopters) measured at each moment in the calculation. By doing this, we are effectively introducing a  $+A$  D lens with a related defocus of  $-A/2$  D. Then, the IOL power calculated by the model is  $-A/2$  D the power which optimizes defocus, which is by definition the circle of least confusion. This corresponds to use averaged corneal power meridians in current IOL power calculations.

The retina is placed at a distance corresponding to the axial length measured for each individual subject. The refractive index for the media is considered as that of the Gullstrand model (1.336) with a dispersion corresponding to water. All calculations are performed in white light, by considering 6 wavelengths between 470 and 700 nm weighted by the spectral sensibility curve under photopic conditions.

In order to select the customized IOL power, from the polychromatic ray tracing performed, the area under the radially averaged polychromatic MTF [32] up to 30 cycles per degree (Eq. (2)) is evaluated for each individual IOL power tested. The numerical integration was also performed using the trapezoidal rule with a step size of 3 cycles per degree.

$$\text{Area\_under\_MTF} = \int_0^{30} \text{radialMTF}(f)df \quad (2)$$

The selected IOL power is that maximizing this image quality metric.

An important feature of this procedure is the ability to use the model to determine the optimum IOL power for different levels of corneal aberrations. This allows to study their impact on the IOL power prediction. We can also modify these aberrations in the same way as the corneal astigmatism is neutralized, using the same surface to add different amount of aberrations to the cornea or compensate for their presence.

## 2.2. Subjects and experimental procedure

In order to illustrate the capabilities of the procedure, we determined the optimum IOL power for 19 healthy subjects covering a wide range of refractive states ( $-1.0 \pm 3.6\text{D}$  of average refractive error with a range from  $-8.5\text{D}$  until  $+4\text{D}$ ). The purpose was to demonstrate the complete IOL power computational procedure as well as to compare the results obtained with those provided by standard regression type IOL power calculations. Consequently, these subjects had not undergone surgery.

The complete set of measurements needed for the prediction was carried out. Three corneal topographies were recorded for every eye in order to study the possible variability and its impact on the IOL power calculation. Axial length and anterior chamber depth were measured with the gold standard for biometry (IOL Master; Carl Zeiss Meditec, Jena, Germany). The predictions obtained by different standard formulas were obtained for comparison. In particular, estimates known as Haigis [8], Hoffer Q [9], Holladay [10] and SRK/T [11] were determined, by using optimized IOL constants for the corresponding IOL model considered for the study that was one aspheric monofocal (Tecnis ZA9003, Abbott Medical Optics, Santa, Ana, CA, USA).

Three personalized eye models were built for each subject considering the three anterior corneal topographies recorded. From these models, the final IOL power was determined with our procedure to be the mode of the three results, due to the fact that IOL powers were selected from those commercially available, that is in  $0.5\text{D}$  steps. Consequently, IOL power retrieved by each paraxial formula was also rounded according to that.

Variability in the calculations due to different topographies was also studied with respect to isolated anterior corneal aberrations computed separately.

## 3. Results

The average, standard deviation and median IOL power over the population are shown in Table 1. All procedures retrieved similar average values. In order to explore the relation between the results retrieved by ray tracing and the rest of approaches, the IOL power resulting for each paraxial formula is plotted as a function of the IOL power calculated by our procedure in Fig. 3. There is a good correlation between different approaches and our method, although it is possible to observe some differences, especially for higher and lower IOL powers.

**Table 1. Predicted IOL power over the population**

Method	Predicted IOL power (D)	
	Mean $\pm$ SD	Median
Custom IOL power	19.69 $\pm$ 4.96	21.25
Haigis	20.19 $\pm$ 4.73	21.75
Hoffer Q	19.81 $\pm$ 4.91	21.25
Holladay I	19.92 $\pm$ 4.66	21.25
SRK/T	19.92 $\pm$ 4.56	21.25

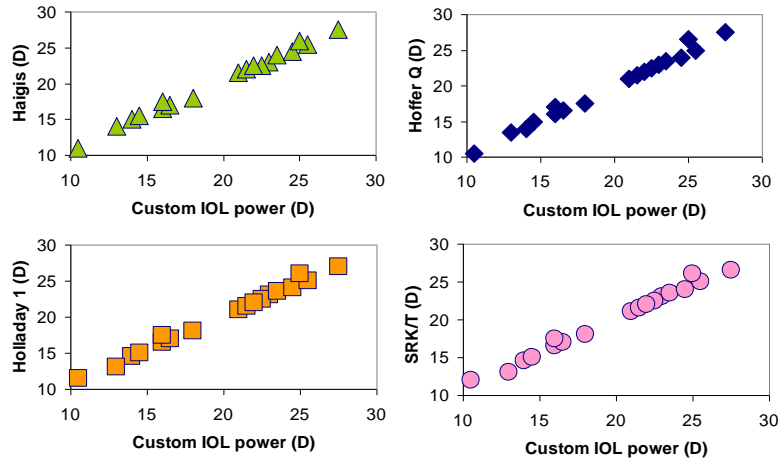


Fig. 3. Scatter diagram showing the IOL power predicted by different paraxial formulas as a function of the result of our customized procedure.

In order to further compare our procedure and the rest of methods considered, we calculated differences between the IOL power predicted by our procedure and the different regression formulas considered in the study. This was done due to the fact that final refraction was unknown because subjects did not undergo surgery and to avoid the bias due to the residual error calculation, that is modulated by the selected method for its calculation. The average difference for all the subjects between the IOL power calculated with our procedure and different regression based formulas is shown in Fig. 4a, together with the average absolute difference (Fig. 4b), in order to consider sign compensations. These figures do not show significant differences on average between the customized procedure and standard calculations. It should be noted that the difference between formulas is also limited on average.

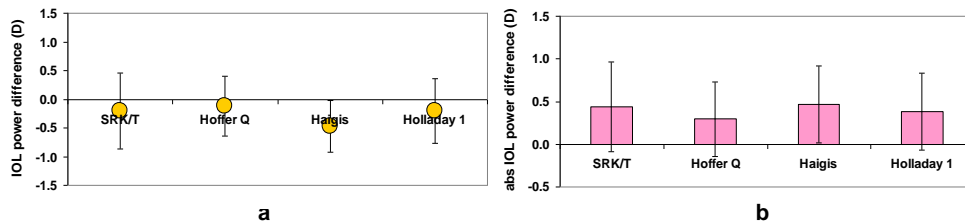


Fig. 4. (a) Average difference between the IOL power calculated by our procedure and different existing formulas for all the subjects included in the study and (b) absolute difference between our procedure and standard formulas.

Figure 5 shows the differences for each subject between the IOL power calculated in the customized eye model and those retrieved by different formulas as a function of the subject's refractive state. For emmetropic eyes, the maximum difference found was 0.5D, which is the step in power for most IOL models available. For these eyes all the formulas provide relatively similar IOL power calculation outcomes, but for myopes and hyperopes the differences increase.

Differences also increase between regression based formulas with increase in refractive error. In order to emphasize this finding, Figs. 6 and 7 show the particular case of ammetropic extremes. As an example, in Fig. 6, the area under the radial MTF as a function of IOL power for the most myopic patient (-8.5D) is shown. In this case, the maximum corresponds to a

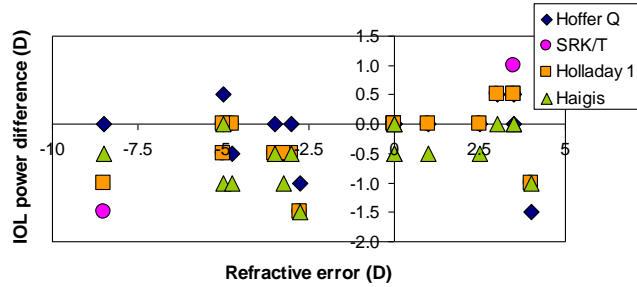


Fig. 5. Difference between the ray tracing prediction and standard IOL power calculations as a function of subject's refractive state.

power of 10.5D, which is the IOL power chosen by the procedure. The different regression formulas predict different IOL power, ranging 10.5D for the Hoffer Q formula, to 12.0 D for the SRK/T formula. The corresponding point-spread functions (PSFs) computed in the eye model for the different IOL powers are also displayed, just as an indication of the optical quality with different IOL powers evaluated.

Figure 7 presents similar information for the most hyperopic eye of the study (+ 4D). In this case, the maximum for the area under the radial MTF is lower than in the previous myopic subject due to higher amount of anterior corneal aberrations (higher order root mean squared (RMS) was  $0.21\mu\text{m}$  compared to  $0.10\mu\text{m}$  for the previous eye, both calculated at 4mm pupil). Due to the discrete sampling in IOL powers, the maximum is found between 24.5D and 25D, so the IOL power chosen for this patient was 25D. The closest prediction for the regression formulas is 1D higher for three of them and 1.5D higher for the Hoffer Q formula.

The differences between the IOL power predicted by the model for each patient and those calculated by the different formulas are plotted in Fig. 8 versus the corneal RMS and higher order RMS calculated for a 4mm pupil. For these eyes, there is no a clear trend relating the differences between IOL power predictions and anterior corneal aberrations.

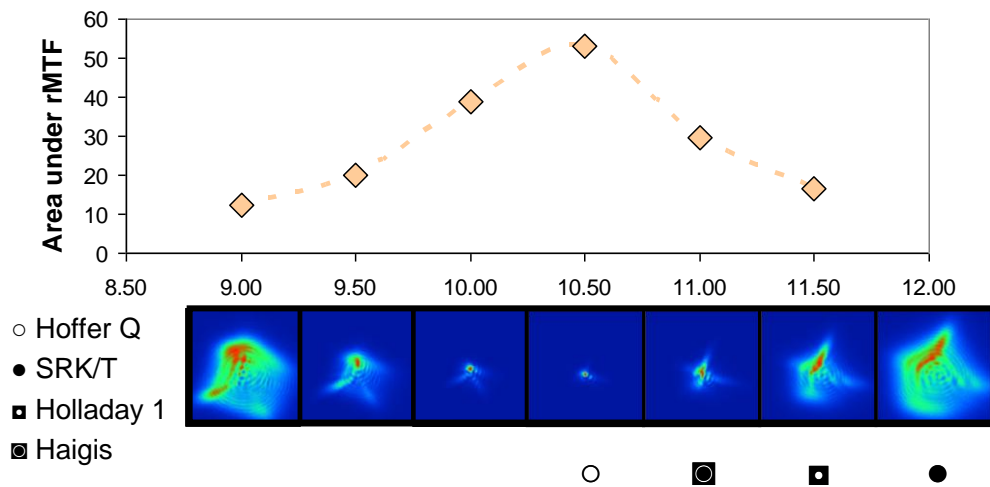


Fig. 6. Most myopic (-8.5D) patient's overview. Top. Area under the radial MTF calculated with the customized model for a wide range of IOL powers. Bottom: PSF retrieved for the same range of IOL powers. Symbols indicate the IOL power retrieved for this patient by different standard calculations.

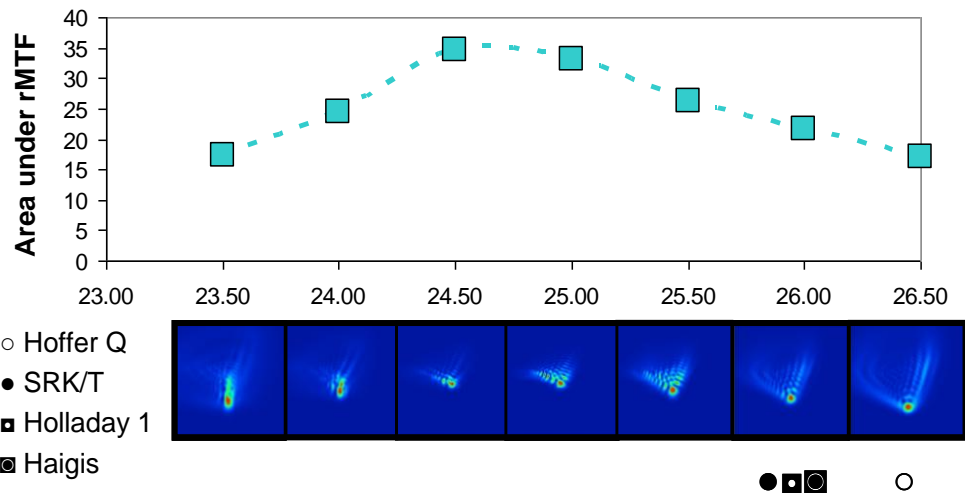


Fig. 7. Most hyperopic (+4.0D) patient's overview. Top. Area under the radial MTF calculated with the customized model for a wide range of IOL powers. Bottom: PSF retrieved for the same range of IOL powers. Symbols indicated the IOL power retrieved for this patient by different standard calculations.

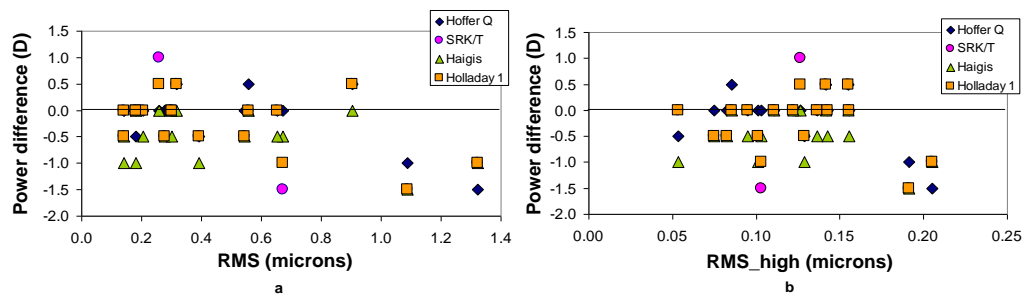


Fig. 8. IOL power differences between the customized ray tracing procedure and standard formulas versus (a) corneal RMS and (b) corneal higher order RMS calculated for 4mm pupil.

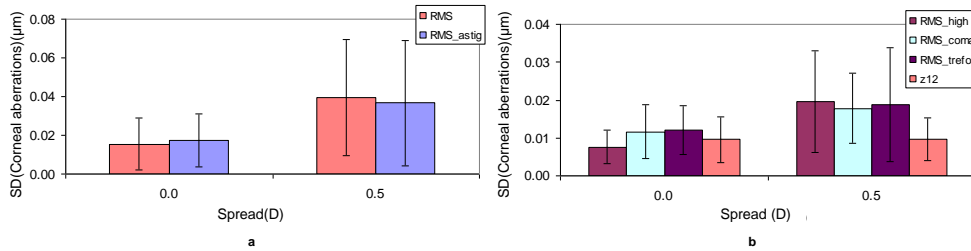


Fig. 9. Standard deviation for different corneal aberrations (a, RMS and astigmatism, and b, higher order RMS, third order coma, trefoil and spherical aberration) for both, the group of subjects with no difference in computed IOL power through the 3 corneal topographies considered and those with 0.5D difference.

The IOL power determined was the mode of the values calculated for each of the three topographies recorded for each patient. The maximum spread between results within one single eye was 0.5D. In order to investigate the reason for this difference, subjects were divided in two groups: those with no deviation in the IOL power calculation prediction

between topographies and those with a 0.5D change among topographies. Figure 9a shows the averaged standard deviation for anterior corneal aberrations RMS (without considering defocus) and anterior corneal astigmatism RMS for both groups. For the group with dispersion, the standard deviation between topographies was higher especially due to corneal astigmatism. Figure 9b shows for both groups, the averaged standard deviation for higher order RMS and different third order aberrations as well as spherical aberration. It can be concluded that these factors are not the cause of the spread in IOL power predictions within eyes, as similar values are shown for both groups. Higher order RMS standard deviation was higher for the group with 0.5D dispersion due to coma and trefoil.

#### 4. Discussion

We present a ray-tracing approach to calculate the optimum IOL power. This approach was previously used to model the optical performance in normal eyes [33,34] and in eyes implanted with IOLs [7,26]. Both studies showed a good correspondence between measured and computed eye's aberrations in a customized eye model that took into consideration the IOL's tilt and decentration. In both cases, all IOL parameters were known, including IOL power used in the surgery as well as its placement in the eye, and tilt and misalignments measured with Purkinje systems. These eye models could be used to model optical performance for new IOLs that correct for the higher order aberrations of the cornea. The impact of the correction of these higher order aberrations can be reduced if the IOL power is not properly chosen. Our aim was to further develop these customized models to be based on preoperative data so that they can be used as a predictive tool.

In addition to monochromatic aberration, polychromatic behavior is also considered in our model. To our knowledge, there is no other IOL power calculation method incorporating this aspect, which may be important for a realistic simulation of the optical quality of the eye. In this direction, recently, the visual impact of correcting chromatic aberrations in IOLs was evaluated [35]. More particularly, it has been shown that the effect of chromatic aberration in pseudophakic eyes is mainly due to IOL material [36]. In order to emphasize the importance of the combined effect between monochromatic and chromatic aberrations in IOL power calculations we had performed the IOL power prediction with our ray tracing procedure in different conditions. The impact of pure chromatic aberration can be seen in Fig. 10, where the IOL power prediction has been performed correcting monochromatic corneal aberrations for the same subject with a virtual IOL model having the same geometrical properties but different Abbe numbers, that is, different chromatic aberration values, both in white light and monochromatic conditions (540nm). As expected, as higher is the Abbe number, there is less difference between both calculations, leading to the same calculated IOL power. In fact, chromatic aberration starts to play a role only for very dispersive, nonrealistic IOL materials, because available commercial IOLs present Abbe numbers between 35 and 60 [36]. The scenario is different when monochromatic aberrations are added to the model and considered in the IOL power prediction (Fig. 11). The polychromatic calculation resembles the effect of chromatic aberration for lower although commercially available IOL's Abbe numbers with lower MTF values, due to the impact of monochromatic aberrations in comparison with the previous calculation where they were corrected (Fig. 10), affecting the selected IOL power. Then, we can conclude that the impact of chromatic aberration is modulated also by monochromatic aberrations. It is important to note that current IOL power calculations do not incorporate dispersion effects and for that reason cannot differentiate between IOL materials.

Former formulas for IOL power calculations are based just in paraxial optics to predict IOL power, with no reference to aberrations that are more often present in the new aspheric IOLs. On the other hand, in older subjects the average pupil under photopic conditions is 3.5mm while in mesopic conditions is 5mm [37]. In both cases, aberrations start to play a role in optical performance, so paraxial optics should not be used. In this study, we decided to use

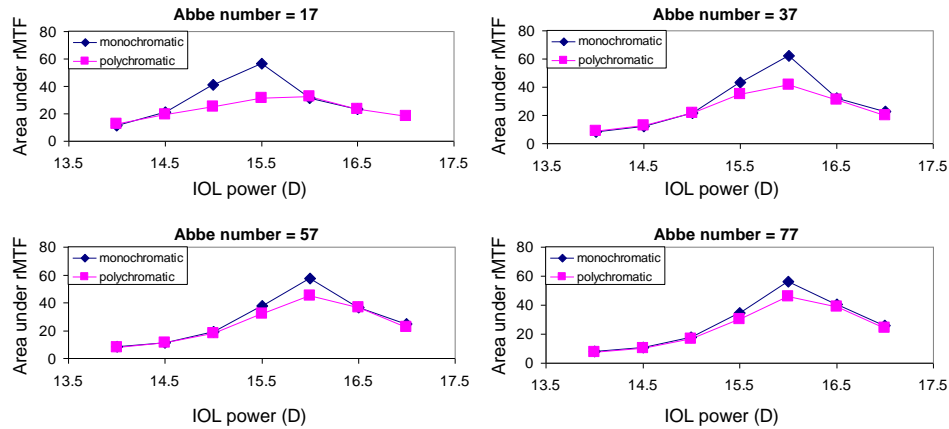


Fig. 10. Area under the radial MTF calculated with our customized procedure, correcting corneal aberrations, as a function of the IOL power with different IOL materials. Therefore, in this plot we show the pure chromatic aberration effect due to the IOL material dispersion.

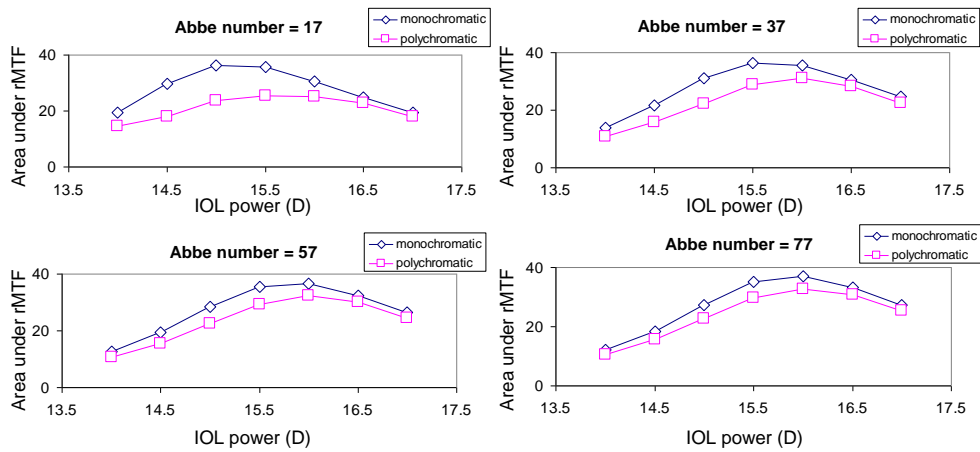


Fig. 11. Area under the radial MTF calculated with our customized procedure, including corneal aberrations, as a function of the IOL power with different IOL materials. Therefore, in this plot we show the combined effect between chromatic aberration due to the IOL material dispersion and corneal aberrations.

4mm pupil since it's realistic under the previous data. However, we didn't find a correlation between the difference with standard regression formulas and our predictions. This may be due to the fact that we included normal eyes that were not highly aberrated. In order to show the importance of the aberrations in IOL power prediction, we chose one subject and we calculated the IOL power with our procedure considering his natural corneal aberrations and with two, three, four and five times the amount of these corneal aberrations (Fig. 12). The IOL power calculated becomes different as higher is the amount of aberrations. Obviously, these changes would not affect the regression formulas due to their paraxial nature. This increase in aberrations might be high but not impossible to find in real eyes. For example, those eyes that had undergone LASIK surgery present increased amounts of corneal aberrations. For them, even the highest level of aberrations used in the example is perfectly possible.

In our approach, the only reference to not personalized data we use is the IOL placement based on a previous found high correlation between the natural lens position and the measured IOL position. The best scenario would be a complete theoretical model only depending on the

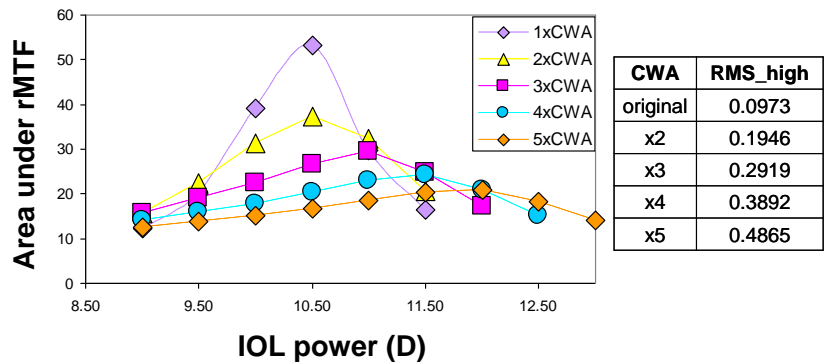


Fig. 12. Area under the radial MTF calculated with our customized procedure as a function of the IOL power for different amounts of corneal aberrations (CWA) referred to 4mm pupil. Their impact on IOL power calculation is studied by increasing the original aberration pattern up to 5 times.

IOL and particular eye's characteristic. This will be the subject of further research to fully customize the model.

It is important to note that because we are using an exact ray tracing procedure, the effective lens position used in paraxial formulas cannot be introduced here. Those authors that have previously studied the IOL power calculation problem with either the thick lens theory or ray tracing have faced the same problem. Olsen [15] or Norrby [38] have developed elaborated actual lens position predictions based on multiple biometric parameters. These or another actual lens position can be introduced in the customized ray tracing procedure that we are presenting in this paper in order to evaluate their accuracy.

In order to evaluate the impact of a different IOL placement prediction on the ray tracing procedure, we repeat the calculations for all the population included in the study by using an ACD prediction recently presented by Norrby et al. [39]. We decided to use this prediction because it has been developed for the same IOL model used here and it includes axial length and anterior chamber depth, which are parameters we measured. Figure 13a shows the relationship between both ACD predictions for all the population of the study ( $r^2 = 0.63$ ). The average difference between both predictions was  $0.11 \pm 0.15$ mm, resulting our prediction in a deeper IOL placement on average than that developed by Norrby et al. It is also well accepted that the ACD prediction is highly correlated with axial length. However, we did not include this parameter in our prediction. In order to explore the impact of axial length in the IOL

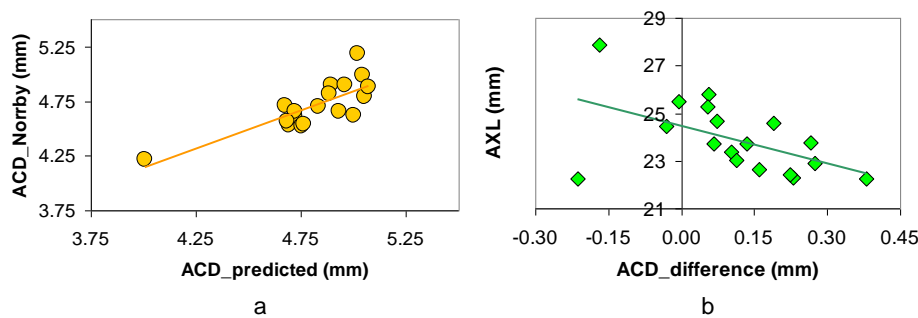


Fig. 13. (a) ACD prediction presented in this paper described by Eq. (1) versus the Norrby prediction [39] for all the study population and (b) difference between both ACD predictions as a function of the axial length.

position prediction, we represent in Fig. 13b the difference between ours and Norrby's approach, which includes the AXL as predictor, as a function of eye's axial length. There is, in fact, a linear correlation between the ACD difference and AXL, although there was some dispersion, leading to a weak correlation between both parameters ( $r^2 = 0.27$ ). Further studies will reveal the method achieving the highest accuracy for the IOL power procedure, although we still believe that a fully theoretical customized procedure for IOL placement is the best approach in order to complete the eye modeling for IOL power calculations.

In order to explore the impact of these differences in the IOL power prediction, we applied the same ray tracing procedure, by generating three customized eye models corresponding to three different corneal topographies per subject, being the selected IOL power the mode of them. Then, the only difference between previous and these results is purely the IOL placement prediction, considered in this case as Norrby et al. [39]. Figure 14 shows the IOL power difference between the ray tracing prediction considering our ACD prediction and Norrby's as a function of the ACD difference. As expected, a deeper IOL placement will lead to a higher predicted IOL power, although there is a range where different ACD placement does not translate to a difference between both predictions. This is due to the fact that we are considering an IOL model with 0.5D steps. However, we did not find an ACD difference value wherein there is a clear step into the higher or lower IOL power. This might be related to the IOL power selection is based on the mode of the results coming from three different corneal topographies, making more complex the results interpretation.

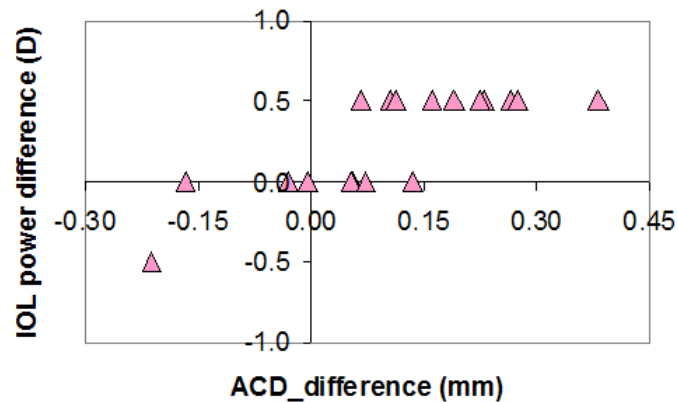


Fig. 14. IOL power difference between ray tracing considering the ACD prediction described by Eq. (1) and that presented by Norrby et al. [39] as a function of the difference between ACD predictions. In both cases, the Norrby's prediction is considered as a reference. Therefore, both the IOL power and ACD differences are our approach minus Norrby's.

It is important to note that although there are differences in the ACD placement, the maximum discrepancy between ray tracing approaches is 0.5D, which is the IOL power step and the variability in the procedure, as we have shown in Fig. 8. In addition, the average IOL power with the Norrby's ACD prediction was  $19.44 \pm 4.84D$  with a median of 21D, the lowest of all the methods considered in the study, including the ray tracing approach with the ACD prediction presented in this paper, as can be seen at Table 1. However, as we had pointed out through the paper, we do not have subject's final refraction results, because they did not undergo cataract surgery. Therefore we can only establish differences between procedures. Further clinical studies will show the most accurate procedure for ACD placement to predict IOL power by ray tracing, although the point of this comparison was also to show the plasticity of the procedure to adopt different ACD predictions.

It is important to note the differences between formulas in a large range of powers for ametropic eyes, establishing also their inaccuracy in those cases. Different solutions have been pointed out in order to increase the accuracy of IOL power calculation considering these formulas, from the modification of the A constants [2], a myopic targeting for an emmetropic outcome or the transformation of axial length measurements to improve refractive outcome in extreme eyes without sacrificing the outcome in normal eyes [40]. However, the regression and paraxial nature remains leading to outliers.

We found that the differences between our calculations and the empirical formulas were higher as greater was the subject's refraction. From this result we only can state the difference but, because subjects didn't undergo actual surgery. Future studies involving actual clinical surgeries could show the absolute differences.

Cataract surgery modifies the cornea by the incision, inducing additional aberrations [41]. Due to the relative low value of these inductions and the tendency to be reduced with time, we believe that the pre-surgery corneal topography provides enough and valid information for the IOL power prediction, although the impact of these changes will be subject of future research.

The introduction of the different biometric parameters in the ray-tracing prediction can be a limit of its accuracy because all the errors involved to those measurements. Norrby [19] quantified the sources of error in IOL power calculations, finding that the most limiting parameter is the IOL placement, followed by the actual determination of the postoperative refraction and the different biometric parameters considered in the calculation. In our case, the variability between topographies showed a maximum difference of 0.5D between power predictions. This variability could be avoided by a prior evaluation of those corneal topographies. Therefore, only those topographies within an astigmatism standard deviation smaller than 0.05 microns should be considered for the IOL power prediction.

Another possible limitation to the procedure is the introduction of a fixed equivalent refractive index to account the power of the posterior corneal. Although there are instruments measuring the posterior corneal surface, we believe that the current model incorporating anterior corneal aberrations provides enough important and valid information without increasing the amount of experimental error in the procedure. Then, the extension of the procedure to consider the posterior corneal is possible, however it would be subject of further research, as well as the modification of the calculated equivalent refractive index for post-LASIK patients.

## 5. Conclusions

We present an optical procedure to estimate the optimum IOL power for a specific lens and individual eye. From biometric measurements, a personalized eye model is built considering a complete representation of the anterior cornea, and then IOL power is determined as that maximizing the area under the polychromatic radial MTF calculated by exact ray tracing. As a proof of concept, IOL power for 19 normal subjects has been calculated and the differences between our results and standard IOL power calculation methods have been analyzed. There was a good agreement between the values provided by both approaches for emmetropic patients, a population that is well known for the accuracy and predictability of standard IOL power estimations. The results are different for subjects with large ametropias, where the differences are also higher between standard regression formulas. This reveals limitations for the current state of art methods of calculating IOL power. Finally, the impact of corneal aberrations was also studied with our procedure, showing more accuracy than standard calculations to predict IOL power, especially in patients with large corneal aberrations, such as those that had undergone refractive surgery and for specific materials with low Abbe number.

## **Acknowledgments**

This work has been supported by “Ministerio de Ciencia e Innovación,” Spain (grants FIS2007-64765, FIS2010-14926), and “Fundación Séneca,” Murcia, Spain (grant 04524/GERM/06). The authors thank Patricia Piers (AMO, Groningen, Holland) for helpful discussions and revision of the manuscript.